

# DISSOLUTION OF CO<sub>2</sub> DROPS AND CO<sub>2</sub> HYDRATE STABILITY UNDER SIMULATED DEEP OCEAN CONDITIONS IN A HIGH-PRESSURE WATER TUNNEL

Robert P. Warzinski<sup>a</sup>, Ronald J. Lynn<sup>a</sup>, Igor Haljasmaa<sup>a</sup>, Yi Zhang<sup>b</sup> and Gerald D. Holder<sup>c</sup>

<sup>a</sup>U.S. Department of Energy, National Energy Technology Laboratory, P.O. Box 10940, Pittsburgh, PA 15236. <sup>b</sup>University of Pittsburgh, Department of Chemical and Petroleum Engineering, 1249 Benedum Hall, Pittsburgh, PA 15261. <sup>c</sup>University of Pittsburgh, School of Engineering, 240 Benedum Hall, Pittsburgh, PA 15261

## ABSTRACT

This paper provides a summary of the current research that is being performed at the National Energy Technology Laboratory on the behavior and fate of carbon dioxide in seawater under conditions simulating direct deep ocean injection. This information is being obtained in a high-pressure water tunnel by observing individual CO<sub>2</sub> drops suspended in a countercurrent flow of water or seawater.

## INTRODUCTION

An accurate assessment of the technological and environmental aspects of any sequestration process depends on the availability of high-quality information on the fundamental physical and chemical behavior of CO<sub>2</sub> in the process. This is particularly true for the deep ocean, which has a large capacity for storing CO<sub>2</sub>, yet also has a potentially high sensitivity associated with perturbations to its environment. It is well known that CO<sub>2</sub> drops injected into the ocean will rise or fall, depending on the injection depth, and that a coating of solid hydrate can form around the CO<sub>2</sub> core.<sup>1,2</sup> In all cases, where the surrounding water is not saturated with carbon dioxide, the carbon dioxide will slowly dissolve in the water, causing the size of the droplet to shrink. The rate of this dissolution is of critical importance. Understanding the formation and stability of hydrate under ocean sequestration scenarios is also important since this substance can have a significant impact on the process.

The National Energy Technology Laboratory (NETL) has been involved in actively performing carbon sequestration research for more than a decade. A significant part of this research has involved experiments on deep ocean sequestration.<sup>3</sup> Early work in this area was performed in small laboratory pressure vessels; however, the need for a device that more realistically simulates the deep ocean environment was evident from the beginning. In 1994, plans for a high-pressure water tunnel were proposed; however, sufficient funding to build such a device was only realized in the past few years as the area of carbon sequestration science began to grow. NETL now has a fully operational, state-of-the-art high-pressure water tunnel facility (HWTF) that is beginning to provide what is hoped will be the most reliable data on important technical issues associated with oceanic sequestration of CO<sub>2</sub>. It is the purpose of this paper to briefly describe this device and to present information on both the dissolution of CO<sub>2</sub> drops under simulated deep ocean conditions and the formation and stability of hydrate shells on the CO<sub>2</sub> drops. When this phase of the experimental research is completed a full report will be published.

## EXPERIMENTAL FACILITY

The development of the HWTF and a companion device, the Low-Pressure Water Tunnel Facility (LWTF), has been the subject of previous reports.<sup>4,5,6</sup> The basic operation of the HWTF with respect to oceanic carbon sequestration is to stabilize a CO<sub>2</sub> bubble, drop or hydrate particle in a countercurrent flow of water or seawater that is automatically controlled to balance the rising or sinking tendencies of the particle. The size, shape and location of the bubble, drop or particle are automatically measured while stabilized. A picture of the HWTF is shown in Figure 1.

Important features of the HWTF include –

- Viewing sections with multiple windows and ports. The main observation windows are polished to near optical flatness to prevent distortion of the image of the particle. The observation windows have a viewing area that is about 4 cm in diameter.
- An automated bubble cap and CO<sub>2</sub> injection system that permits the introduction of fluid particles of various sizes. The maximum particle size in the current configuration is about 2 cm in diameter; however, particles reported in this paper were generally less than 1.5 cm in initial diameter. A separate flushing pump can also be used to purge the CO<sub>2</sub> injection line with water or seawater if required.
- Well characterized flow conditioning elements that provide the necessary velocity profiles to stabilize the particle in the main observation window while preventing contact of the particle with the walls or windows of the vessel. Velocity profiles were initially chosen to allow as much natural motion of the particle to occur in the HWTF as possible.
- A fully automated particle control system that tracks the position of the particle and utilizes pump speed and flow bypass to regulate the position of the particle in the desired location. This system allows operation of the HWTF with minimal intervention.
- A fully automated particle measurement and data acquisition system that records particle movement in all three dimensions. This provides for a detailed record of the particle motion in the HWTF. This system also measures the size of the particle from two orthogonal positions which allows for correction of any parallax effects as the drop moves with respect to the camera on the main observation window. When the particle is in the observation window, information on its position and size are collected 25 times a second. Typical experiments involve stabilizing a particle for about 30 minutes to 50 minutes, depending on the size of the particle and the dissolution rate. During this time the size, shape and location of the particle are monitored and recorded and the aqueous flow rate required to stabilize the particle is measured.
- Automatic temperature and pressure control to within 0.1 °C and 7 KPa, respectively. These values are recorded every minute using a precision digital Heise gauge and platinum resistance thermometers (RTDs).
- A semi-automated data processing system that provides a summary of changes in particle size and shape, dissolution rate, particle position and process conditions.

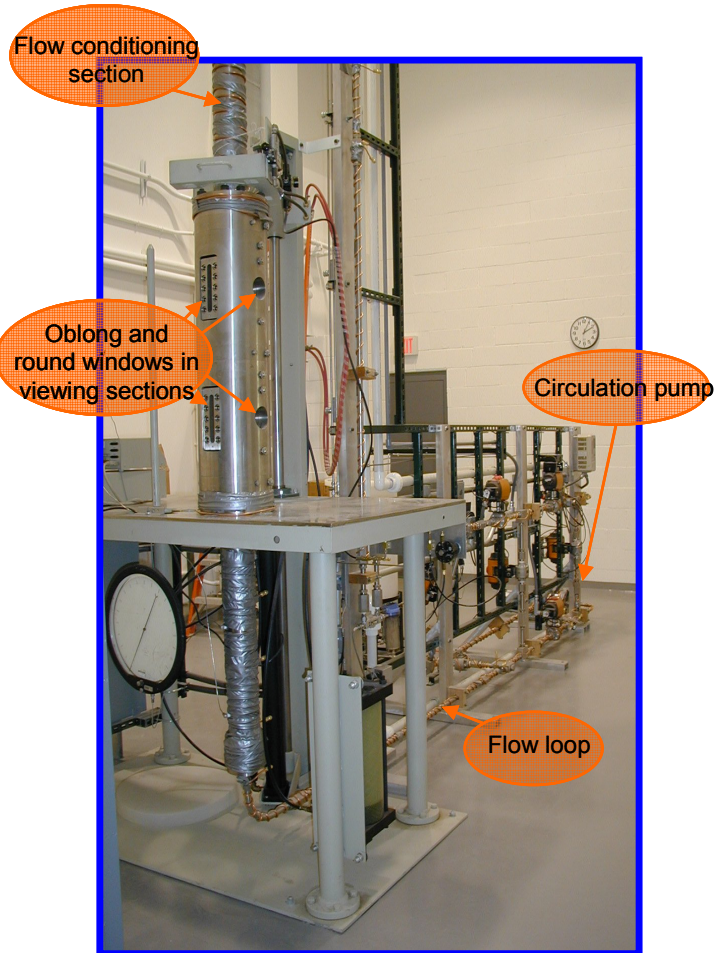


**Figure 1.** High-Pressure Water Tunnel at NETL (without insulation).

While initially designed and built for oceanic sequestration research, the HWTF can be used to study the behavior of particles in any fluid system that is compatible with 316 stainless steel and Hastelloy C. Pressures to 34.5 MPa are possible. Other possible applications include natural gas hydrates and the behavior of CO<sub>2</sub> in geologic saline formations.

The data reported in this paper were obtained using 99.999% purity CO<sub>2</sub> and either water purified by reverse osmosis (RO) and activated carbon filtration or an artificial, 35-salinity seawater prepared following the recipe given by Millero.<sup>7</sup> Hereafter in this report the terms RO water and seawater will refer to these media.

## EXPERIMENTAL RESULTS

### Drop Dissolution

A data set using both RO water and seawater was obtained in 2003 during initial operation of the HWTF. Based upon this initial period of operation, significant improvements were made to both the flow system and associated control software, and to the particle measurement and tracking system that improved the quality of the data. Experiments have recently resumed and a second set of data is being obtained in RO water and seawater over a range of temperatures, pressures, and dissolved CO<sub>2</sub> content that includes those anticipated for deep ocean sequestration. The data for RO water are summarized in Figure 2. Seawater data are also being obtained and will be reported at the conference.

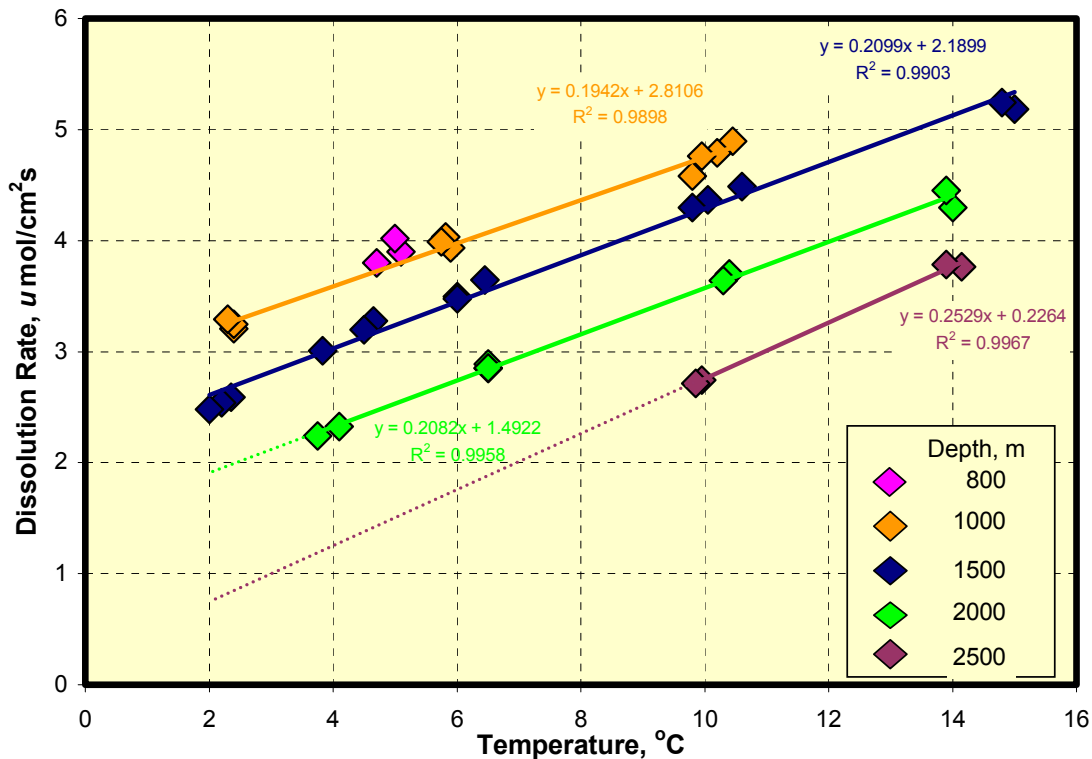


**Figure 2.** Dissolution of CO<sub>2</sub> in RO water as a function of temperature and depth.

Figure 2 shows the dissolution rate of positively buoyant CO<sub>2</sub> drops as a function of temperature and pressure which is expressed as equivalent depth (100 m = 1 MPa). These data indicate that the rate of dissolution decreases with depth. The reason this occurs is that the particle density of CO<sub>2</sub> increases with depth. As it becomes closer to the value of water the buoyancy and therefore the rise velocity decrease. Thus, the velocity of water required to stabilize the particle decreases with depth. Since dissolution from the surface of the bubble is directly correlated with the velocity of the water flowing past the particle (rise velocity), greater depths produce lower dissolution rates. Interestingly, this means that a particle injected at depth, i.e. 2500 meters, would initially rise slowly and dissolve slowly, but the further it rose, the faster it would rise and the faster it would dissolve.

The dashed extensions of the regression lines in Figure 2 show the regions where the CO<sub>2</sub> drops were denser than the water. (Note that these lines should not be used for extrapolation of the data.) After collection of similar data for seawater is completed the HWTF will be reconfigured to collect information on sinking drops.

The data at 800 meters and 4.7°C to 5.1°C in Figure 2 were obtained to compare to previous data obtained by Brewer et al., in the Pacific Ocean at 800 m, 4.4°C.<sup>8</sup> They obtained a dissolution rate of 3.0  $\mu\text{mol}/\text{cm}^2\text{s}$  which is slightly lower than the value of 3.9  $\mu\text{mol}/\text{cm}^2\text{s}$  obtained in the HWTF. Also, the HWTF value is for RO water. The seawater value may be slightly lower. The hydrodynamic conditions in the HWTF also are not exactly like those in Brewer's *in-situ* measurement channel and could likely result in a higher dissolution rate. An indication of this difference is observed in the average rise rate of the drops. For Brewer's drop, the initial rise rate at 804 m was 10.2 cm/s; for our drops it was about 12.5 cm/s (as calculated from the flow measurements and velocity profile expected in the HWTF). This difference is nearly proportional to the observed difference in the dissolution rates.

The drop shrinkage rates used to calculate the results in Figure 2 are also similar to those determined by Teng and Yamasaki<sup>9</sup> in a similar countercurrent flow device in artificial seawater; however, no hydrodynamic details are available for their device. Also, their dissolution data do not follow the nearly linear trend with respect to temperature that is observed in Figure 2. A closer comparison of the two data sets will be made when our seawater data set is completed.

### Hydrate Formation

An important goal of the research at NETL has been to study drop dissolution at conditions necessary for hydrate formation and stability. Our previous research in small windowed pressure vessels was among the first to highlight the importance of dissolved  $\text{CO}_2$  content in these processes.<sup>3, 10, 11</sup> This work showed that at 2°C and 17.5 MPa, a dissolved  $\text{CO}_2$  concentration of 4.9 wt% was necessary for formation of a stable hydrate shell in General Purpose Seawater of 35 salinity from Ocean Scientific International, Ltd.

Experiments were performed in the HWTF at 1500 m simulated depth to investigate the conditions of temperature, pressure, and dissolved  $\text{CO}_2$  content on hydrate shell formation and stability. In experiments with water, no hydrate shell formation was observed over the temperature range of 2°C to 15°C in RO water with no dissolved  $\text{CO}_2$  or in RO water with 2 wt% dissolved  $\text{CO}_2$ . However, at 4 wt%  $\text{CO}_2$  a stable hydrate shell was formed on the drop during injection that persisted throughout its dissolution. The presence of the shell decreased the dissolution rate by about an order of magnitude. This is shown in Figure 3 along with similar results from experiments in seawater.

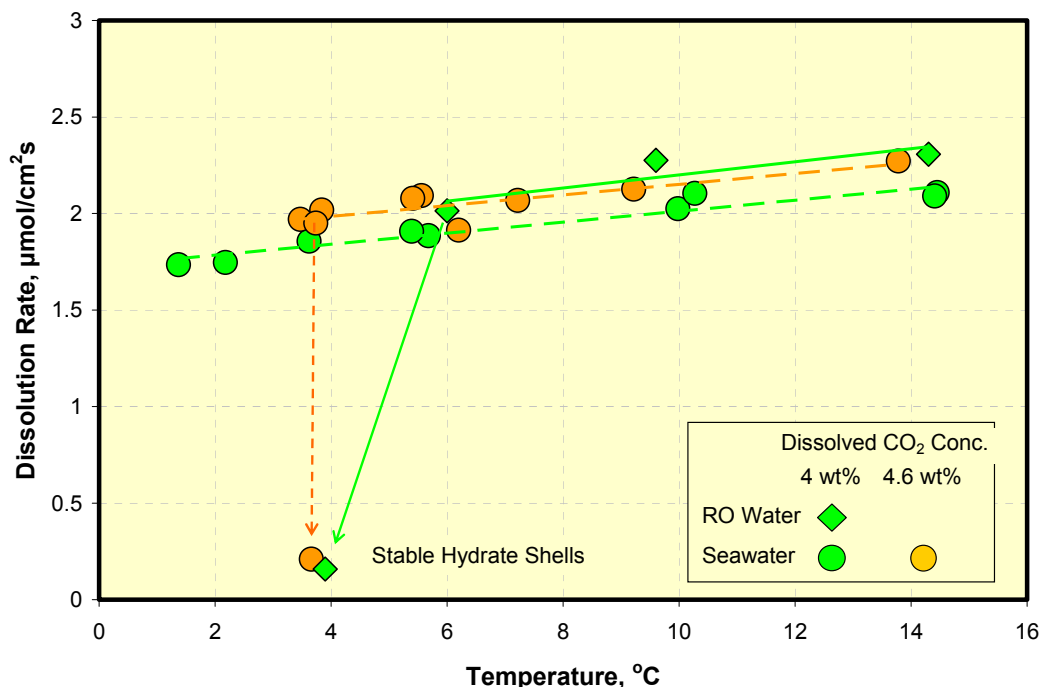


**Figure 3.** Dissolution of  $\text{CO}_2$  in RO water and seawater at 1500 m with sufficient  $\text{CO}_2$  dissolved in the water to promote the formation of a stable hydrate shell.

In seawater, a 4 wt% concentration of dissolved CO<sub>2</sub> did not promote the formation of a stable hydrate shell; however, increasing the concentration to 4.6 wt% did. In this case, the equilibrium point appeared to be close to 3.5°C as evidenced by the drops that did not form a shell at nearly the same temperature. For RO water the equilibrium point was between 3.9°C and 6°C at 4 wt% CO<sub>2</sub>. For thermodynamic reasons, it is anticipated that the equilibrium point for stable hydrate shell formation will vary with temperature, depth and salinity. Experiments in the HWTF will be performed to obtain such information.

Prior theoretical models and observations in laboratory experiments at NETL indicated that the hydrate shell that initially forms on a CO<sub>2</sub> drop thins with time.<sup>2, 12</sup> This observation has been confirmed in the HWTF. A hydrate covered drop (the one formed in RO water at 3.9°C) is shown in Figures 4a and 4b at approximately 1 min and 43 min, respectively, after injection.

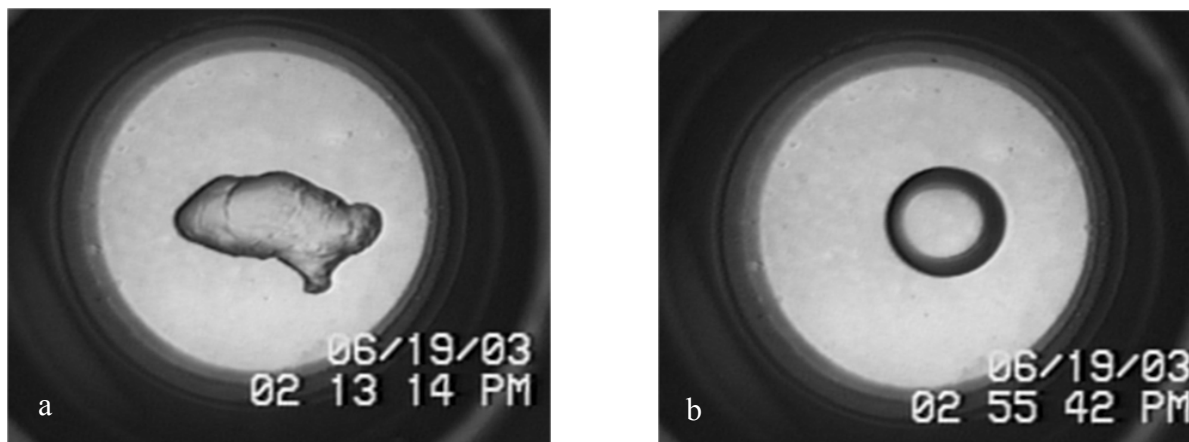


**Figure 4.** Images of a hydrate covered drop at 1500 m, 3.9°C, in water with 4 wt% dissolved CO<sub>2</sub>. Images were taken at (a) 1 minute and (b) 43 minutes after injection.

The hydrate shell that formed was initially very rough and strong enough to maintain the non-spherical particle shape. Within 4 minutes the drop had assumed a nearly spherical shape. Some remnants of the shell were still visible at 4 minutes; however, as shown in Figure 4b any visual evidence of the shell had vanished at 43 minutes. This indicates that the presence of a hydrate shell may not be easily discerned by visual observation alone. In the case of this drop, the continuing presence of the hydrate shell was evident in the dissolution rate data which did not change throughout the observation period, even though some thinning of the shell was visually evident. Without hydrate, the dissolution rate would have been much higher. The continuing presence of a hydrate shell could also be inferred from the lack of any momentary deformity (no wobbling) in the shape of the drop as it moved within the viewing region.

Theoretical considerations suggest that the lower dissolution rates observed when hydrates are present are due to the lower solubility of CO<sub>2</sub> in the water when hydrates are present. When hydrates are present, the solubility corresponds to the solubility at the three-phase hydrate equilibrium pressure which is much lower than the system pressure. When no hydrates are present, the CO<sub>2</sub> solubility is governed by the system pressure and is much higher. General mass transfer principles require that the rate of dissolution be determined by the *difference* between the concentration at the surface of the particle and the bulk.<sup>13</sup> If the surface concentration is determined by the solubility and the solubility is lower when hydrates are present, the rate of mass transfer and dissolution will be lower when hydrates are present. Using this model, virtually the same mass transfer coefficient is obtained with and without hydrates. A more detailed description of these calculations is being prepared for publication.

## CURRENT RESEARCH

As of this writing, experiments are continuing to obtain dissolution data on CO<sub>2</sub> drops in seawater as a function of temperature, depth, and dissolved CO<sub>2</sub> content. Particular attention will be given to the region of hydrate stability. The HWTF will also be reconfigured to stabilize sinking particles. This primarily

involves changing the positions of the automated drop injection system and release cap and the video tracking and measurement systems. Under these conditions the data sets will be extended to 3500 m.

## ACKNOWLEDGMENTS

The authors would like to acknowledge Charles Levander and Jerry Foster for their efforts in implementing the HWTF.

## DISCLAIMER

Reference in this paper to any specific product, process or service is to facilitate understanding and does not imply its endorsement or favoring by the U.S. Department of Energy.

## REFERENCES

- 
- <sup>1</sup> Holder, G. D.; Cugini, A. V.; Warzinski, R. P. *Environ. Sci. Tech.*, **1995**, *29*, 276-278
  - <sup>2</sup> Holder, G. D.; Warzinski, R. P. *Prepr. Pap., Am. Chem. Soc., Div. Fuel Chem.*, **1996**, *41(4)*, 1452-1457.
  - <sup>3</sup> Holder, G. D.; Mokka, L. P.; Warzinski, R. P. *Chem. Eng. Sci.* **2001**, *56*, 6897-6903.
  - <sup>4</sup> Warzinski, R. P.; Lynn, R. J.; Robertson, A. M.; Haljasmaa, I. V. *Prepr. Pap., Am. Chem. Soc., Div. Fuel Chem.*, **2000**, *45(4)*, 809-813.
  - <sup>5</sup> Warzinski, R. P.; Lynn, R. J.; Robertson, A. M.; Haljasmaa, I. V. *Prepr. Pap., Am. Chem. Soc., Div. Fuel Chem.*, **2002**, *47(1)*, 25-26.
  - <sup>6</sup> Haljasmaa, I. V.; Vipperman, J. S.; Lynn, R. J.; Warzinski, R. P. *Rev. Scientific Instruments*, submitted.
  - <sup>7</sup> Millero, F. J. *Chemical Oceanography*, 2<sup>nd</sup> Ed.; CRC Press, Inc.: Boca Raton, Florida, 1996; 67.
  - <sup>8</sup> Brewer, P. G.; Peltzer, E. T.; Friederich, G.; Rehder, G. *Environ. Sci. Technol.* **2002**, *36*, 5441-5446.
  - <sup>9</sup> Teng, H.; Yamasaki, A. *Energy Conversion & Management* **2002**, *41*, 929-937.
  - <sup>10</sup> Warzinski, R. P.; Cugini, A. V.; Holder, G. D. In *Coal Science*; Pajares, J. A.; Tascón, J. M. D., Eds.; Elsevier Science Ltd.: Amsterdam, The Netherlands, 1995, 1931-1934.
  - <sup>11</sup> Warzinski; Holder, G. D. In *Greenhouse Gas Control Technologies*; Riemer, P.; Eliasson, B.; Wokaun, A., Eds.; Elsevier Science Ltd.: Amsterdam, The Netherlands, 1999, 1061-1063.
  - <sup>12</sup> Warzinski, R. P.; Lynn, R. J.; Holder, G. D. *Gas Hydrates: Challenges for the Future*; Holder, G. D.; Bishnoi, P. R., Eds.; Annals of the New York Academy of Sciences, Vol. 912; The New York Academy of Sciences, New York, 2000, 226-234.
  - <sup>13</sup> Ogasawara, K.; Yamasaki, A.; Teng, H. *Energy & Fuels*, **2001**, *15*, 147-150.